NUCLEAR SCIENCE AND ENGINEERING: **181**, 1–8 (2015)

The Impact of Neutron Cross Section Group Structures on the Accuracy of Radiological Source Models

A. P. J. Hodgson*

AWE plc, Aldermaston, Reading, Berkshire, RG7 4PR, United Kingdom

and

Department of Materials, Imperial College London, Royal School of Mines Exhibition Road, London, SW7 2AZ, United Kingdom

R. W. Grimes and M. J. D. Rushton

Department of Materials, Imperial College London, Royal School of Mines Exhibition Road, London, SW7 2AZ, United Kingdom

and

O. J. Marsden

AWE plc, Aldermaston, Reading, Berkshire, RG7 4PR, United Kingdom

Received December 19, 2014
Accepted March 9, 2015
http://dx.doi.org/10.13182/NSE14-156

Abstract—*Computational models provide a framework through which to predict impurity in-growth in reactor generated radiological sources. However, the energy group structure and methodology used in these codes can have a significant impact on the accuracy of neutron cross sections and, as a result, on the inventory values calculated. The European Activation SYstem II (EASY-II) partitions neutron data in a number of different standard structures and then uses these to generate energy collapsed cross sections for each neutron reaction of interest. How well these single values represent the true neutron environment of the reactor is key to the codes efficacy for evaluating source impurities for use in material attribution. By comparing EASY-II nuclide inventories for cobalt source materials against analytically derived equivalents, these approximations have been shown to have limited impact. However, of the fission applicable standard structures investigated, only XMAS and CCFE were capable of precisely accounting for the differences in the energies required to simulate all the neutron reactions of potential interest to forensic investigations.*

I. INTRODUCTION

The production rate of a given nuclide within reactor generated radiological materials is dependent on: the reactor's neutron flux, the cross sections of the neutron reactions, the atom density of the target nuclide, and the irradiation time. The energy dependence of these interactions, together with the unique nature of reactor neutron flux spectra, means that different reactor types will produce materials with varying levels of reactor generated impurities. With the potential for the illicit use of such materials growing, these nuclide impurities could

*E-mail: a.hodgson11@imperial.ac.uk

assist law enforcement officers in distinguishing between different material production routes and locations.[1] Understanding how these impurities alter with reactor environment and the manufacturing processes used is therefore key to identifying which nuclides could be utilised as forensic signatures in the evaluation of materials of unknown provenance.

Computational approaches provide a powerful tool with which to model these environments.[2,3] A number of different methods are available, which differ with respect to the codes utilised and the style of simulation used.[4–7] The European Activation SYstem II (EASY-II), which is developed and maintained by the Culham Centre for Fusion Energy (CCFE), is one such approach and is capable of modelling activation, transmutation, and burn-up resulting from nuclear interactions with matter.[8] The program's underlying code, FISPACT-II, undertakes multi-pulse irradiation calculations, together with extensive uncertainty and sensitivity analyses. EASY-II therefore provides an internationally recognised and validated standard through which to model signature development.

As a deterministic code, FISPACT-II makes a number of assumptions to enable solutions to the problems with which it is presented, such as presuming the target material to be homogeneous, infinite, and infinitely dilute; and assuming that the projectile flux is not modified by the reactions and decays within the target material.[8] The most pertinent though, is the approximations made to reaction cross sections. Energy independent values are generated for each reaction of interest by collapsing multigroup libraries down into single values. As neutron cross sections are highly energy dependent, ensuring that these cross sections accurately represent the reaction environment underpins the confidence that users have in the results produced. To achieve this, it is therefore important to address not only the accuracy of the cross sections themselves, but also if the compatibility of the group structures within EASY-II is sufficient to define each reaction of interest across the neutron energy range.

Here, the impact these approximations have on the development and precision of thermal reactor generated radiological source inventories is assessed. Neutron flux spectra, based on an MCNP6 model of the TRIGA Mark III–type Thai Research Reactor (TRR-1), are partitioned into a number of thermal reactor energy group structures compatible with the FISPACT-II code.[9,10] These flux spectra are then used in EASY-II to compute energy collapsed cross sections and material inventory values for cross comparison, and are also evaluated against results produced using a standard analytical approach to inventory calculations.

II. ENERGY GROUP STRUCTURES

There are two basic approaches to using cross sections: continuous energy and multigroup. For many deterministic codes, such as EASY-II, providing a continuous energy solution would be computationally expensive. Numerical approximations are therefore made where point-wise cross sections are averaged over specific energy ranges to form multigroup cross sections σ_g using the expression[11]

$$\sigma_g = \frac{1}{\phi_g} \sum_{i=0}^{n+1} \int_{E_i}^{E_{i+1}} \phi(E)\sigma(E)dE \ , \qquad (1)$$

where

$\phi(E)$ = one of five weighting functions (flat, $1/E$, Maxwellian thermal, fission spectrum, or velocity exponential fusion)

$\sigma(E)$ = cross section

ϕ_g = value of the weighting function integrated over the group

E_i = energy of the i'th point.

A large number of energy groups in a cross section library can improve the accuracy of the calculations performed, but will increase the computational overhead; a compromise must therefore be established.

European Activation File (EAF-2010) and TALYS based TENDL-2011 and TENDL-2012 evaluated nuclear data libraries are included as part of EASY-II (Refs. 12, 13, and 14). These are provided in a variety of different energy group structures, calculated using SAFEPAQ-II, for use depending on the application and the energy spectrum of the irradiating flux.[11] As structures applicable to fission applications, the LANL, WIMS, GAM-II, XMAS, and CCFE energy groups are the most applicable to applications involving thermal reactor generated radiological sources. Each grouping is designed to take into account four important physical phenomena in the reactor: the generation of fission neutrons, neutron slowing and diffusion, resonance absorption, and neutron thermalization. The energy ranges can therefore be divided into three main regions: fast, resonance, and thermal. All five group structures differ slightly in the extent to which these regions are represented (see Table I), and it is these variations that can have an impact on the extent to which the cross sections cause activation and/or transmutation of nuclides within the material being modelled.

III. SOURCE SIGNATURES

There are several well documented events where radiological sources have left regulatory control, and in so doing have helped substantiate the belief that such materials could potentially be exploited for malicious intent.[15,16] The majority of the radioactive material used in radiological

TABLE I

Overview of a Selection of Fission Applicable Energy Group Structures Supported by FISPACT-II*

Name	Number of Energy Groups				Maximum Neutron Energy (MeV)
	Thermal	Epithermal	Fast	Total	
LANL	23	18	25	66	25.00
WIMS	42	13	14	69	10.00
GAM-II	10	31	59	100	14.92
XMAS	80	47	45	172	19.64
CCFE	280	168	261	709	1000.00

* References 8 and 23 through 27.

sources is generated in nuclear reactors via one of two main methods: neutron activation of elemental targets, or fission/activation of actinide materials. Sources that are produced from stable target materials are of particular forensic interest, because these materials are generally not available carrier free. Impurities generated during the irradiation process therefore remain embedded in the source material produced—as there is no need for any post production processing—and so these can potentially be used as indicators of the material's irradiation history.

Radiative capture reactions, otherwise known as (n,γ) reactions, are essential in the transmutation of the stable elemental targets into their radioactive equivalents. Despite these reactions being possible across the neutron energy range, they occur predominantly at thermal energies. Reactors are therefore set up to maximise the moderation of fission neutrons down to thermal energies. However, a significant proportion of neutrons are still present at higher energies. These neutrons can induce non-elastic neutron absorption reactions that result in the emission of charged particles, such as protons or alpha particles, or the release of excess neutrons. Reactions such as these may not occur at any specific energy range, but can be prevalent at certain resonances. When modelling source production, the differences in the neutron energies necessary to induce these reactions need to be accurately reflected in the energy group structure chosen, as any discrepancies will directly impact the extent and manner in which these impurities are accounted for.

Most reactor generated radionuclides are not believed to pose a security threat, because of their very short or very long half lives. Those that do, tend to be radioactive materials of commercial value with half lives ranging from a few days up to ~1000 years. Based on this fact, there are approximately a dozen radionuclides deemed as being of greatest security concern, and of these, only two, ^{60}Co and ^{192}Ir, are manufactured directly from stable elemental targets.[17] When looking for a model system to evaluate the differences in how each group structure (see Sec. II) predicts the production of potential forensic signatures, the monoisotopic nature of cobalt targets, ^{59}Co, is ideal. Nickel and iron are the main impurities produced during cobalt irradiations, primarily by radiative capture and non-elastic neutron interactions, respectively, and so are the elements used here to assess group structure suitability.

IV. INVENTORY CALCULATIONS

IV.A. EASY-II

The evolution of inventory nuclides within the FISPACT-II code is centred around a series of rate equations[18]:

$$\frac{dN_i}{dt} = \sum_j \left(\lambda_i^j + \sigma_i^j \phi^{int}(t)\right) N_j \ , \tag{2}$$

where

N_i = number of nuclide i present at time t

ϕ^{int} = projectile flux

λ_i^j = decay constant of nuclide j producing i

σ_i^j = reaction cross section for the reactions on j that produce i, when $j \neq i$; when $j = i$, $-\lambda_i^j$ is the total decay constant of nuclide j and $-\sigma_i^j$ is the total cross section for all reactions on j that produce i.

The process shown in Eq. (2) can also be thought of as the sum of a number of paths and loops, otherwise known as pathways. FISPACT-II therefore analyses these pathways based on digraph methods using the DLSODES solver, which is the double-precision variant of the LSODE package developed at the Lawrence Livermore National Laboratory.[19,20]

The reaction cross sections used in these calculations are dependent on the projectile energy, the source data, and the energy structure employed. In the code, effective single value cross sections are therefore generated from the multigroup nuclear data libraries and the neutron flux spectra provided using Eq. (3):

$$\sigma_i^j = \sum_n \sigma_i^j(E_n)\phi(E_n) \Big/ \sum_n \phi(E_n) \ , \tag{3}$$

where

$\sigma_i^j(E_n)$ = cross section at neutron energy n

$\phi(E_n)$ = integrated neutron flux in energy group n

and where the sums are over all energy groups.

By computing the data in this manner, FISPACT-II is able to weight the library values, using the neutron flux spectrum, to generate energy independent values. How well these single point values represent the true neutron environment will depend on the type of cross section being evaluated (continuous or threshold) and the type and extent of the energy group structure being employed.

IV.B. Analytical Approach

When both the neutron flux and the cross sections of a given material are known, the number of reactions R for a particular neutron interaction in any given time interval t, can be calculated based on Eq. (4):

$$R = N V t \sigma \phi \,, \tag{4}$$

where

N = atom density

V = material volume.

Generating simulations for a given material where the number of reactions for all potential interactions are calculated in series, means that it is possible to use these expressions to enable real-time updates of the material's elemental and isotopic composition; provided the time interval used is small enough to accurately account for any short-lived radioactive constituents. However, if the neutron flux and cross sections used are stored according to the energy defined group structures described above, then Eq. (4) can be better represented by

$$R = \sum_n N V t \sigma(E_n) \phi(E_n) \,, \tag{5}$$

where the impact that cross sections, and their associated neutron flux, have on the inventory values of each nuclide within the material can be assessed for each neutron energy E_n within the multigroup structure. Such expressions are able to more precisely account for cross sectional variations across the energy range, and thus can be used to assess the accuracy of the energy independent values generated by FISPACT-II.

A simple Python based program, centred on these expressions, was therefore developed to account for all neutron reactions essential for the production and loss of cobalt, iron, and nickel isotopes during source production. Models are run for a stated irradiation time, and inventory values are updated at the end of every time interval during that period. To aid cross-comparison, the code makes the same assumptions as those previously stated for EASY-II, and also utilises the EAF-2010 and TALYS libraries for all nuclear data values.

V. METHODOLOGY

V.A. Neutron Flux

The open source MCNP model of TRR-1, developed by Gallmeier et al., was used to provide reactor fluxes and their associated uncertainties.[10] The core consists of 121 reactor element positions in a hexagonal grid, containing: 67 standard fuel elements, 38 low-enriched uranium fuel elements, 3 neutron detector elements, 8 empty irradiation positions, 4 boron carbide control rods, and a trim rod.

MCNP6 (MCNP6 v1.0) track-length estimated FMESH tallies were used to derive the average neutron flux for the reactor's whole fuel region based on each of the energy group structures previously stated.[9] The neutron fluxes were calculated with KCODE runs corresponding to the reactor when fully loaded with fresh fuel at a working control rod configuration using ENDF/B-VI.1 cross sections, and operating with a coolant and cladding temperature of 293.6 K and a fuel temperature of 600 K. The results were then scaled to the steady state thermal power of the reactor using a nominal reactor power of 1.2 MW and an effective multiplication factor k_{eff} of 1.08252 ± 0.00025 (Refs. 21 and 22). The results of these calculations, in units of flux per MeV, are shown in Fig. 1; the overall statistical uncertainty of the simulations was $<5\%$.

V.B. Radionuclide Inventory

FISPACT-II inventory calculations were performed using LANL, WIMS, GAM-II, XMAS, and CCFE energy-defined neutron flux spectra, for an irradiation time of 2 years and a stated total neutron flux of 2.629×10^{13} n·cm^{-2}·s^{-1}. In addition to these parameters, the analytical method also required a time interval between inventory updates, which was set at 100 s. Both methods utilised neutron cross sections and decay data that were generated using either EAF-2010, as was the case for the LANL, WIMS, GAM-II, and XMAS group structures, or for the 709-group CCFE structure, TENDL-2012. The target material was based on a standard ^{59}Co pellet of 1-mm diameter and length, presumed to be free from all impurities, as tends to be stated by manufacturers.

V.C. Uncertainty

Uncertainty estimates were generated using FISPACT-II where pathway analysis was used to identify the pathways from the initial inventory nuclides that lead to the production of the dominant nuclides at the end of the irradiation phase. For each dominant nuclide

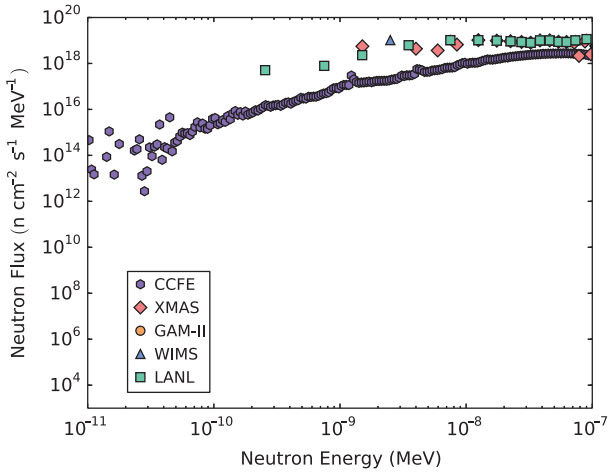

(a)

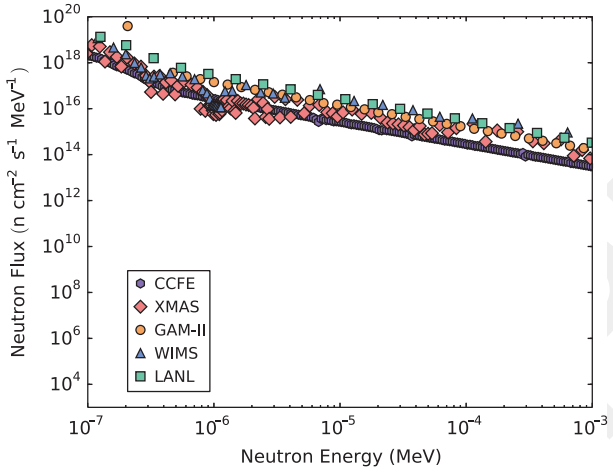

(b)

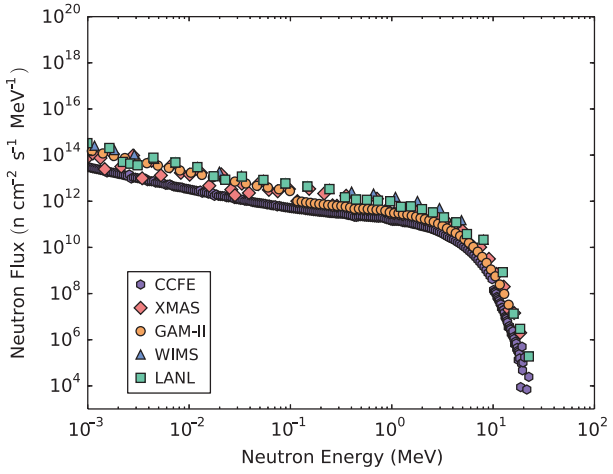

(c)

Fig. 1. Monte Carlo derived neutron flux spectra for the fuel region of TRR-1 at (a) thermal, (b) epithermal, and (c) fast neutron energies.

identified, the number of atoms created due to the reaction and decay chain along each path to that nuclide was recorded. Together with the uncertainties in the reaction cross sections and decay half lives for each pathway, FISPACT-II used this information to generate the total associated statistical uncertainty with 1 σ confidence intervals.[8] These estimates were then used on both FISPACT-II and analytically calculated inventory values, as the cross section and decay data used in each instance were the same.

VI. RESULTS AND DISCUSSION

VI.A. Radiative Capture Reactions

How well the energy group structure and analysis technique chosen are able to represent the true cross section directly impacts the accuracy of the nuclide inventory values calculated. Figure 2 indicates that FISPACT-II is able to generate highly comparable inventory values for radiative capture products in cobalt targets for nearly all potential energy group structures. The main exception is GAM-II, which overestimates atom production compared to the other FISPACT-II values. For nuclei early in the radiative capture chain, such as ^{60}Co (see Fig. 2a) which is generated directly from the ^{59}Co target, these values are still within the uncertainty of the other FISPACT-II calculations. However, moving further down the neutron capture chain, to nuclei such as ^{61}Ni (see Fig. 2b), the lack of overlap in the error bars indicates a significant difference between the values generated.

The reason for this discrepancy is the minimal thermal energy range representation in GAM-II, where a single energy group is used to account for all neutron energies below 0.41 eV (Refs. 23 and 24). As a consequence of this, the thermal components of both the cross section and neutron flux are exaggerated. When FISPACT-II then uses these values to generate the energy collapsed cross section, the neutron flux skews the weighting of the cross section value towards this minimally represented energy region, overestimating the value calculated (see Table II). This is not too great a concern when looking at single stage transmutations or short irradiation times, but for extended radiative capture chains, this systematic overestimation will lead to inconsistencies. For GAM-II generated analytical answers however, the atom numbers are underestimated. This is a direct consequence of the inaccurate representation of the radiative capture cross section in the thermal energy range. In this instance though, as the individual cross sections for each energy group are being used—rather than the energy collapsed value generated by FISPACT-II—the mid–energy range value for this large grouping underestimates the thermal contribution.

The analytical results in general correlate well with the FISPACT-II answers, especially when using the WIMS, XMAS, and CCFE group structures. This

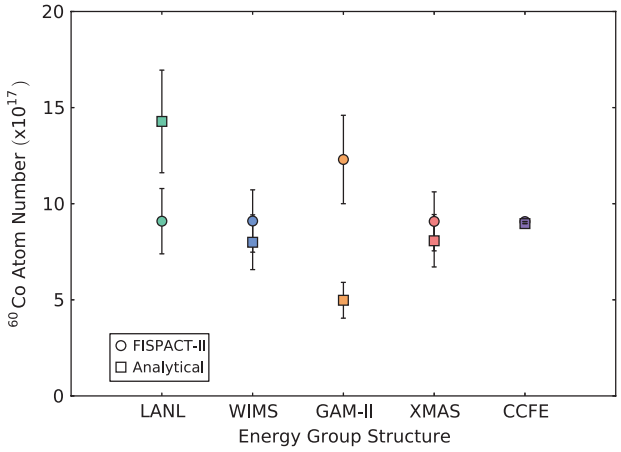

(a)

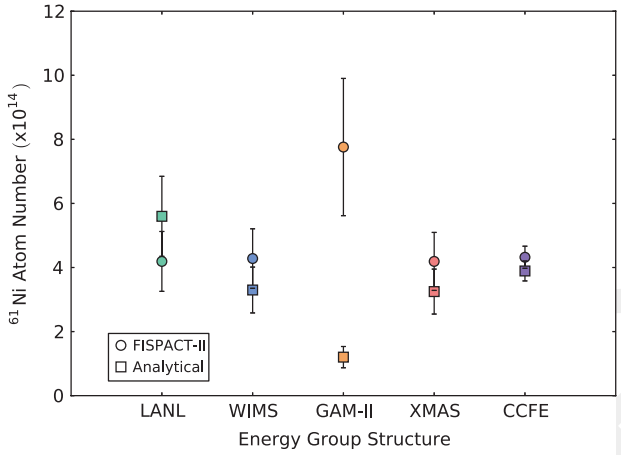

(b)

Fig. 2. Energy group defined nuclide inventory values for radiative capture dominated (a) ^{60}Co and (b) ^{61}Ni production during the irradiation of a stable cobalt pellet.

TABLE II

FISPACT-II ^{59}Co $(n,\gamma)^{60}$Co Energy Collapsed Cross Sections

Energy Structure	Cross Section (b)
LANL	3.9093
WIMS	3.9149
GAM-II	5.3216
XMAS	3.9063
CCFE	3.2876

substantiates the ability of energy collapsed cross sections to accurately represent radiative capture cross sections, provided that the correct energy structure is employed. This is illustrated in Fig. 2 by the variation in the accuracy of the LANL analytical results produced with respect to FISPACT-II. The divergence seen is a result of how the group structure accounts for the resonance region of this reaction. As indicated in Fig. 3, LANL generates a significantly larger value for the main resonance peak of the ^{59}Co$(n,\gamma)^{60}$Co cross section than WIMS, GAM-II, and XMAS, which all have relatively similar energy group boundaries and/or structures. This inconsistency makes very little difference to the FISPACT-II result, as the weighting of the other 65 energy group values masks this single incorrect value. However, for the analytical calculation this is not possible, and this erroneous cross section has a direct impact on the final value generated.

When choosing an energy group structure, it is therefore important to address not only how well the structure represents the cross section but also the way in which it is going to be employed within the calculations performed.

VI.B. Non-Elastic Neutron Absorption

For the vast majority of nuclides, the impurities produced by non-elastic neutron absorption show strong agreement in FISPACT-II regardless of the energy group structure employed and are also well correlated with their analytically generated equivalents (see Fig. 4a). This is even the case for GAM-II, as the higher energy required for these interactions offsets the group structure's limited thermal representation. This conformity again highlights the accuracy that can be produced by the energy collapsed cross sections used in FISPACT-II. The correlation shown by both radiative capture and non-elastic neutron absorption interactions also indicates that the differences in the neutron energies of these various interactions do not impact on the precision of the cross section produced.

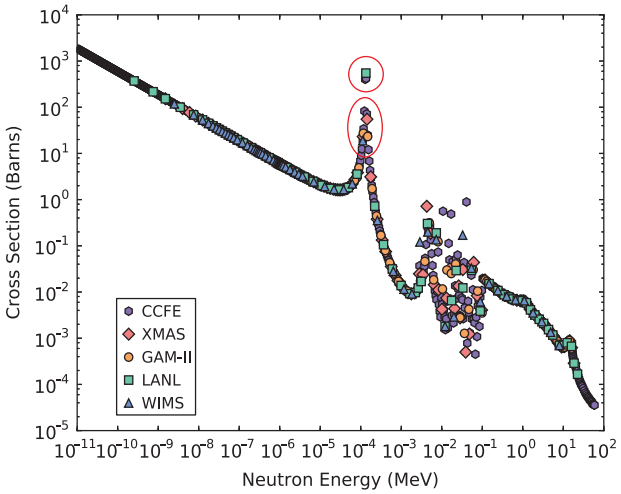

Fig. 3. Comparison of the ^{59}Co$(n,\gamma)^{60}$Co neutron cross section with respect to energy group structure. The circles indicate the variation of the resonance peak value between the LANL, WIMS, and XMAS group structures.

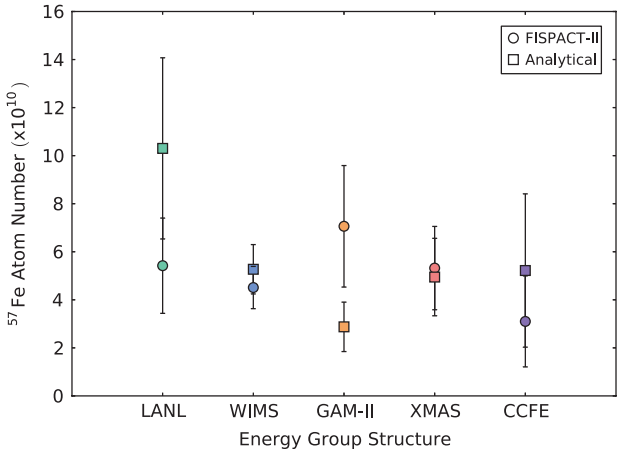

(a)

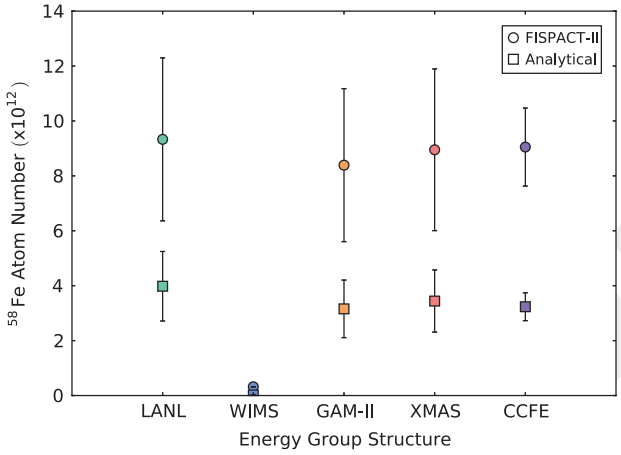

(b)

Fig. 4. Non-elastic dominated energy group defined nuclide inventory values for (a) ^{57}Fe and (b) ^{58}Fe production during the irradiation of a stable cobalt pellet.

There is, however, more variation between the answers illustrated in Fig. 4 than that seen in the reactions dominated by radiative capture (see Fig. 2). This is to be expected, because as a large proportion of these impurities are induced by threshold and resonance specific interactions they will be more sensitive to the positioning of the energy group boundaries, as averaging about the threshold will influence the accuracy of the neutron cross section generated. This issue is highlighted by ^{58}Fe, where there is a considerable difference between the values generated by WIMS and the other group structures (see Fig. 4b). Iron-58 production is dominated by the reactions ^{59}Co$(n,n+p)^{58}$Fe, ^{59}Co$(n,d)^{58}$Fe, ^{60}Co$(n,t)^{58}$Fe, ^{61}Ni$(n,\alpha)^{58}$Fe, and ^{62}Ni$(n,n+\alpha)^{58}$Fe. Most of these interactions are threshold reactions, which only occur at higher neutron energies that start at, or around, 10 MeV; the maximum neutron energy accounted for within WIMS (see Table I). Calculations involving WIMS are therefore not able to accurately estimate the neutron cross sections of these reactions and their contribution to ^{58}Fe production (see Table III). Normally, this would not be of great concern, due to the small impact these threshold reactions have compared to the more dominant continuous energy interactions. However, because of the extended irradiation period involved in ^{60}Co production, and the fact that a number of these reactions involve the most abundant nuclides within the target material (^{59}Co and ^{60}Co), these discrepancies become exaggerated and so inhibit the ability of the group structure to reflect the true neutron environment of the reactor.

VII. CONCLUSIONS

The use of energy collapsed neutron cross sections in EASY-II, has little influence on the ability of the software to estimate the neutron environment experienced within thermal reactors compared to energy dependent values. Nevertheless, when using these models to assess radiological source materials for potential forensic signatures associated with impurity in-growth, the energy group structure that is utilised is key because both radiative capture and non-elastic neutron absorption interactions need to be accurately accounted for. The majority of energy group structures compatible with EASY-II, and applicable to fission applications, are shown to have limitations in this respect. Only the XMAS and CCFE group structures are able to cope well with the differences in the neutron energies required for the various neutron interactions within cobalt targets. There is also strong correlation between the nuclide inventory values generated by the two multigroup structures; the only major difference being the reduced uncertainties associated with the 709 groups of CCFE. It should be noted though that these evaluations have only been performed on cobalt cross sections and those of its associated impurities. XMAS and CCFE groupings both have strong representation across the neutron energy range and so should be able to accurately account for cross sections of relevance to any potential target material. However, due to the unique nature of neutron cross sections, it would be prudent to utilise the CCFE group structure for all

TABLE III

FISPACT-II ^{59}Co$(n,n+p)^{58}$Fe Energy Collapsed Cross Sections

Energy Structure	Cross Section (b)
LANL	2.5163×10^{-5}
WIMS	2.2626×10^{-6}
GAM-II	2.5060×10^{-5}
XMAS	2.5270×10^{-5}
CCFE	2.7870×10^{-5}

potential forensic investigations until a more thorough assessment has been made of the source material being evaluated.

ACKNOWLEDGMENTS

The TRR-1 MCNP model used in this research was kindly provided courtesy of Oak Ridge National Laboratory, U.S. Department of Energy. The authors are also grateful to AWE plc for the financial support provided to this project.

REFERENCES

1. "IAEA Nuclear Security Series No. 6—Combating Illicit Trafficking in Nuclear and Other Radioactive Material," STI/PUB/1309, International Atomic Energy Agency (2007).

2. D. KONTOGEORGAKOS, F. TZIKA, and I. E. STAMATELATOS, "Neutron Activation Study of the GRR-1 Research Reactor Core Supporting Plate," *Nucl. Technol.*, **175**, 435 (2011); http://dx.doi.org/10.13182/NT175-435.

3. H. EZURE, "Survey of Estimation Methods for Radioactive Inventory in Nuclear Reactors to be Decommissioned," *J. Nucl. Sci. Technol.*, **35**, 379 (1998); http://dx.doi.org/10.1080/18811248.1998.9733875.

4. W. B. WILSON et al., "A Manual for CINDER'90 Version 07.4 Codes and Data," LA-UR-07-8412, Los Alamos National Laboratory (2008).

5. R. F. BURSTALL, "FISPIN: A Computer Code for Nuclide Inventory Calculations," ND-R-328(R), UKAEA Risley Nuclear Power Development Establishment (1979).

6. S. T. WEINSTEIN, "NAC: Neutron Activation Analysis and Product Isotope Inventory Code System," NASA TM X-52460, National Aeronautics and Space Administration (1968).

7. J. SANZ, O. CABELLOS, and N. GARCIA-HERRANZ, "ACAB Inventory Code for Nuclear Applications: User's Manual V," NEA-1839/02, OECD Nuclear Energy Agency (2008).

8. J. C. SUBLET, J. W. EASTWOOD, and J. G. MORGAN, "The FISPACT-II User Manual Issue 4," CCFE-R(11)11, Culham Centre for Fusion Energy (2013).

9. J. T. GOORLEY et al., "MCNP6 User's Manual, Version 1.0," LA-CP-13-00634, Los Alamos National Laboratory (2013).

10. F. X. GALLMEIER, J. S. TANG, and R. T. PRIMM, III, "MCNP—Model for the OAEP Thai Research Reactor," ORNL/TM-13656, Oak Ridge National Laboratory (1998).

11. L. W. PACKER and R. A. FORREST, "SAFEPAQ-II: User Manual 8th Edition," CCFE-R(10)03, EURATOM/CCFE Fusion Association (2010).

12. L. W. PACKER and J. C. SUBLET, "The European Activation File: EAF–2010 Decay Data Library," CCFE-R(10)02, EURATOM/CCFE Fusion Association (2010).

13. A. J. KONING and D. ROCHMAN, "Modern Nuclear Data Evaluation with the TALYS Code System," *Nucl. Data Sheets*, **113**, 2841 (2012); http://dx.doi.org/10.1016/j.nds.2012.11.002.

14. A. J. KONING and D. ROCHMAN, "TENDL-2011; TALYS-Based Evaluated Nuclear Data Library" (2011); www.talys.eu/tendl-2011 (current as of Dec. 19, 2014).

15. "Strengthening Control over Radioactive Sources in Authorized Use and Regaining Control over Orphan Sources," IAEA-TECDOC-1388, International Atomic Energy Agency (2004).

16. R. TRAGER, "Hunt for Stolen Radiotherapy Unit," *Chem. World*, **11**, *2*, 1 (2014).

17. C. D. FERGUSON, "Ensuring the Security of Radioactive Sources: National and Global Responsibilities," US-Korea Institute at SAIS (2012).

18. H. BATEMAN, "The Solution of a System of Differential Equations Occurring in the Theory of Radioactive Transformations," *Proc. Cambridge Philos. Soc.*, p. 423 (1910).

19. K. RADHAKRISHNAN and A. C. HINDMARSH, "Description and Use of LSODE, the Livermore Solver for Ordinary Differential Equations," UCRL-ID-113855 / NASA RP-1327, National Aeronautics and Space Administration (1993).

20. A. C. HINDMARSH, "Brief Description of ODEPACK—A Systematized Collection of ODE Solvers-Double Precision Version" (2001); http://www.netlib.org/odepack/opkd-sum (current as of Dec. 19, 2014).

21. L. SNOJ and M. RAVNIK, "Calculation of Power Density with MCNP in TRIGA Reactor," *Proc. Int. Conf. Nuclear Energy for New Europe*, p. 109.1 (2006).

22. G. ŽEROVNIK, M. PODVRATNIK, and L. SNOJ, "On Normalization of Fluxes and Reaction Rates in MCNP Criticality Calculations," *Ann. Nucl. Energy*, **63**, 126 (2014); http://dx.doi.org/10.1016/j.anucene.2013.07.045.

23. D. G. CACUCI, *Handbook of Nuclear Engineering Vol. 1: Nuclear Engineering Fundamentals*, Springer Science and Business Media (2010).

24. G. D. JOANOU and J. S. DUDEK, "GAM-II: A B3 Code for the Calculation of Fast Neutron Spectra and Associated Multigroup Constants," GA-4265, General Atomics (1963).

25. J. R. ASKEW, F. J. FAYER, and P. B. KEMSHELL, "A General Description of the Lattice Code WIMS," *J. Brit. Nucl. Eng. Soc.,* **5**, 564 (1966).

26. M. S. SPERGEL et al., "Cosmogenic Neutron-Capture-Produced Nuclides in Stony Meteorites," *J. Geophys. Res.*, **91**, D483 (1986); http://dx.doi.org/10.1029/JB091iB04p0D483.

27. E. SARTORI, "Standard Energy Group Structures of Cross Section Libraries for Reactor Shielding, Reactor Cell and Fusion Neutronics Applications: VITAMIN-J, ECCO-33, ECCO-2000 and XMAS," JEP/DOC-315 Rev. 3, Nuclear Energy Agency (1990).